Desalination and Water Treatment
www.deswater.com

doi: 10.5004/dwt.2017.20122

62 (2017) 1–10
February

Experimental investigation of a solar powered humidification-dehumidification desalination unit

Sirine Saidi[a,d,*], Rym Ben Radhia[a,b], Brahim Benhamou[c], Naima Nafiri[c], Sadok Ben Jabrallah[a,d]

[a]*Laboratory of Energy, Heat And Mass Transfer, University of Tunis El Manar, 1060 Tunis, Tunisia, Tel. +216 25 832 801; email: sirine274@live.fr*
[b]*College of Science at Yanbu, Tbaiah University, Saudi Arabia, Tel. +9660148618888; Fax: +9660143222459; email: rymo2001@yahoo.fr*
[c]*EnR2E, National Center Studies and Research on Water and Energy (CNEREE) & LMFE (CNRST Associated Research Unit URAC27) Faculty of Sciences Semlalia, Cadi Ayyad University, Marrakech, Morocco, Fax: +212 524 43 74 10; emails: B.Benhamou@uca.ma (B. Benhamou), nafiri@uca.ma (N. Nafiri)*
[d]*Faculty of Sciences of Bizerte, University of Carthage, 7021 Bizerte, Tunisia, Tel. +216 98 486 708; Fax: +216 72 590 566; email: sadok.jabrallah@fsb.rnu.tn*

Received 2 February 2016; Accepted 27 July 2016

ABSTRACT

The present work deals with an experimental study of a solar desalination unit using the humidification-dehumidification (HDH) process. A bench-scale desalination unit was designed and tested in Bizerte, Tunisia. Humidification is achieved through a humidifier with saline water falling on its absorber plate, and dehumidification is realized by means of a tubular heat-exchanger condenser. The desalination unit operates with open-water and open-air cycles. Thermal performances as well as fresh water production of the HDH desalination unit were evaluated via measurements of air and water temperatures and flow rates. Measurements were conducted in free and forced convection. Special attention was focused on the influence of air velocity on the fresh water production of the desalination unit. The optimal air velocity, corresponding to the maximum of fresh water production, was found to be 3.34 m/s.

Keywords: Solar energy; Desalination; Humidification; Dehumidification; Water film; Free convection; Forced convection

1. Introduction

Resources in fresh water in the world are facing the demographic growth and the increase of the needs more and more insufficient, and they are increasingly threatened by any sort of pollution [1]. This is particularly the case in MENA region and especially in Maghreb countries (Tunisia, Morocco, Mauritania, Libya and Algeria) [2–4]. On the other hand, in these countries, solar energy resources are abundantly available, and people live mostly in coastal areas. Thus, solar energy powered desalination systems are suitable there [5].

Membrane and distillation processes, such reverse osmosis (RO) or multi-stage flash (MSF), are interesting for large and medium capacity fresh water production [5], as these technologies are expensive, are energy intensive and require high-quality maintenance. Energy consumption of these standards technologies are around 10 kWh/m^3 for MSF and 3 kWh/m^3 for RO [6]. On the other hand, the humidification-dehumidification (HDH) desalination process is a suitable choice for low fresh water needs and areas with decentralized demand. HDH is a low-temperature process where total required thermal energy can be obtained from solar. Capacity production of HDH desalination units is between membrane/distillation units and solar stills. It should be noted that the predecessor of the HDH cycle is the simple solar still. The main drawback of the solar still is

* Corresponding author.

that the processes of solar absorption, evaporation, condensation and heat recovery occur within a single component. This leads to low efficiency (gained output ratio [GOR] less than 0.5), which is primarily the result of the immediate loss of the latent heat of condensation through the glass cover of the still.

In the HDH system, solar absorption, evaporation, condensation and heat recovery processes are separated into distinct components. This separation is the essential characteristic of the HDH system, which operates using air as a carrier gas to shuttle vapor and energy between the evaporation and condensation processes. The simplest HDH desalination unit consists of three subsystems: (a) the air and/or the water heater, which can be solar thermal energy powered; (b) the humidifier and (c) the dehumidifier or the condenser. HDH systems may be classified based on the form of energy used, the cycle configuration or the type of heating used. Energy source in HDH units is a low-grade one, which can be provided by renewable resources (solar thermal, geothermal etc.). Air cycle in a HDH system may be open or closed. In open-air cycle, air is heated, humidified and partially dehumidified and let out in an open cycle. In the opposite, air is circulated in a closed loop between the humidifier and the dehumidifier in a closed-air cycle. The type of heating used in HDH unit is water or air heating systems. The performance of the system depends greatly on whether air or water is heated [7].

Many studies, both theoretical and experimental, are available in the literature on HDH desalination. Narayan et al. [7] reviewed recent studies on HDH desalination systems. Comparison of thermal performance as well as fresh water production of these systems was performed by the authors. Narayan et al. [8] conducted an experimental investigation for the optimization of a pilot-scale HDH desalination unit with a peak production capacity of 700 l/d. The authors concluded that mass extraction from the humidifier to the dehumidifier increases the GOR of the water-heated, closed-air, open-water HDH system by up to 55%. The authors claim that their pilot unit achieves a maximum GOR of 4, by means of this mass extraction. Nawayseh et al. [9,10] conducted numerical and experimental investigations on a solar HDH desalination system. Three units of different sizes (two pilot-scales and one bench) were constructed and tested by the authors in Jordan and Malaysia. Each unit is constituted by a flat solar water collector, an air closed loop with wooden slats cooling tower humidifier and a condenser. Two configurations of the condenser were tested. The three units were also operated in a steady state mode using an electrical water heater in order to perform well-controlled measurements and study heat and mass transfer in the units. Air was circulated in the closed loop either by natural draft or forced convection. Authors derived heat and mass transfer coefficients from experiments for both the humidifier and the condenser [9]. Through computer resources, authors studied the effect of the feed water and air flow rates [10]. Their results showed a weak effect of air flow rate on mass transfer coefficients in the wooden slats cooling tower humidifier, in contrast to a significant effect of the feeding water flow rate. The optimal value of the latter was found to be 0.01 $kg.s^{-1}$, which yields to 2.75 $kg.m^{-2}/d$ of fresh water production [10]. This is explained by the two opposite effects of increasing feed water flow rate, as it leads to a higher solar collector efficiency but lowers evaporation efficiency. Dai and Zhang [11] studied a solar HDH desalination system experimentally. Their experimental device is composed mainly of a water solar collector, a honeycomb packed material humidifier and a tubular condenser with open-air and closed-water cycles. The experimental tests have been made in forced convection. The authors noted that the performance of the system depends strongly on the feeding water temperature and flow rate. The optimal value of air flow rate was determined at two different salt water temperature at the humidifier inlet. The authors showed that thermal efficiency of the system defined by the ratio of the amount of useful energy to total heat input per unit time per unit surface to receive solar irradiation is of about 85% in the optimum operating conditions. Nafey et al. [12,13] examined experimentally the effects of the flow rate of feed water in the humidifier, the air velocity, the flow rate of cooling water in the dehumidifier and the solar flux on a solar HDH desalination system in Egypt. The device is constituted by two solar air and water collectors, a humidifier and a dehumidifier. The authors developed a correlation to predict the production of the unit under different operating conditions. Orfi et al. [14] conducted a numerical and experimental study of a solar-driven HDH desalination system composed by two solar water and air flat collectors. The experimental study was taken place in Monastir (Tunisia) and involves measurements of temperature and humidity at the inlet and the outlet of different components of the desalination system. The theoretical results show that the fresh water production vs. feed airflow exhibits an optimum value. Yamale and Solmus [15] conducted series of measurements on a solar HDH desalination system in Turkey. The device is constituted by a solar air collector, a humidifier and a dehumidifier. The results of the experimental study showed that under some conditions of exploitation, the system production decreases by about 15% if the air solar collector is not used. A significant improvement in the system production is achieved by increasing the temperature of the water inside the storage tank and the cooling water flow rate. The results obtained from this study were compared with the theoretical investigation and good concordance was observed. Marmouch et al. [16] carried out a theoretical study to test a cooling tower as humidifier on the production of a solar HDH desalination. The device is the same as in [14] except for the humidifier. The numerical results show that the studied unit can produce fresh water at high rates of 37 $l.m^{-2}/d$ by introducing the cooling tower while the production of the system is too close to 15 $l.m^{-2}/d$ otherwise. Wang et al. [17] conducted an experimental study on a solar-driven HDH desalination system in China. The authors showed that the system yield is improved by forced convection. They also noted that the desalination unit production increases as the temperature of the cooling water decreases and the temperature of the feed water increases. Recently, Kabeel et al. [18] conducted an experimental investigation of a closed-air and open-water cycles solar HDH desalination unit in Egypt. Brackish water is heated through a solar collector and sprayed on cellulose paper packing material at the top of the humidifier. The closed-air cycle consists of saturated air, circulated by either natural or forced convection, which leaves the humidifier from its top and enters a cylindrical shell heat

exchanger condenser unit from its top. The cooling fluid is cold brackish water, which is circulated inside copper coil with corrugated fins. The authors studied the effects of four parameters on the desalination unit performance: water temperature at the humidifier inlet (T_{hwi}), the mass flow rates ratio of cooling to hot water (C/H), the cellulose paper packing material and three positions of the fan in the case of forced convection (up, down and up-down). The authors found that the best performance corresponds to forced convection from down (fan at the humidifier entrance), with T_{hwi} = 90°C, C/H = 2 and 4 kg.min^{-1} for hot water flow rate. The optimum production obtained was 23.6 kg.h^{-1} of distillated water. One of the interesting results is that the production of the desalination unit running in up-down forced convection mode (2 fans, one at the humidifier entrance and the other at its exit) is similar to the buoyancy-driven convection. Yildirim et al. [19] studied experimentally a HDH desalination system that functions in open-air and open-water loops. It is composed by a humidifier and a condenser. Measurements were devoted to the determination of the inlet and outlet temperatures of the condenser, the production and the coefficient of performance (COP) during the day. The study showed that the maximum daily production of the system is of 143.6 g and the maximum value of the COP is of 0.78. The authors explained that the fresh water production is rather weak because of the low value of the inlet water temperature at the humidifier and the weak exchange surface of the condenser (0.192 m^2). Tahri et al. [20] studied numerically a condenser of a solar desalination unit HDH. The condenser used is composed of 302 parallel tubes disposed vertically. The resolution of the energy and mass balances has allowed to test the influence of operating parameters on the production system. They showed that the production increases with the relative humidity and air flow rate. On the other hand, the increase of the cooling water temperature and the water flow rate in the humidifier has a negative effect on the production. Niroomand et al. [21] studied numerically a desalination system by HDH, which is composed by a humidifier and a dehumidifier. In the system, the air is dehumidified by pulverization cold water into the hot humid airflow. The mathematical model used is based on energy and mass balances. The authors studied the effects of temperatures and flow rates of hot and cold water and droplet diameters on the system production. They showed that the system production increases with the increase in the flow and the diameters of the droplets in the dehumidifier and the water temperature in the humidifier and decreases with the increase of the cooling water temperature. The increase of the air flow rate improves the evaporation but has a negative effect on condensation.

As far as Tunisian experimental work is concerned, in addition to references [14,16], many other researchers conducted investigations on different configurations of solar-driven HDH desalination systems. One of these interesting studies is that carried out by Zhani et al. in Sfax (Tunisia) [22–24]. The studied system is composed of solar air and water flat collectors, a cooling tower type evaporator and a plate heat exchanger condenser. The experimental investigation concerns the dynamic behavior of the solar desalination unit during summer. Measurements concern time evolution of air and water temperature and relative humidity at the inlet and the outlet of each component of the system. The authors show that the maximum fresh water production obtained was 20.5 kg/d on 16th July 2009 for a 16 and 12 m^2 solar air and water collectors, respectively [22].

In light of the above literature review, a HDH solar powered desalination bench-scale unit was constructed and tested in the Bizerte group of the LETTM Laboratory located in the city of Bizerte, Tunisia (37.3° latitude, 9.9° longitude). It is constituted of a humidifier in addition to a tubular condenser. In a previous paper [25], we investigated the performance of the humidifier. In this paper, we studied experimentally the complete desalination unit composed by a humidifier connected to a tubular condenser. The main objective of the present study is to test the desalination unit in real conditions. Specifically, the effect of some parameters such as the type of air draft (natural or forced), air velocity and the climate parameters on the desalination fresh water production is investigated. The optimal air velocity, corresponding to the maximum of fresh water production, is determined in this study.

2. Experimental setup and procedure

Figs. 1 and 2 show the desalination unit. Its main components are a humidifier and a tubular condenser. The desalination unit consists of three independent open-air and open-water loops. Two of them are for the cooling water and the salt water, and the third is for air. Air is circulated either by natural or by forced flow. Airflow goes up through the humidifier, where it is in direct contact with a falling water film. Air is then simultaneously heated and humidified following the evaporation of the film subject to solar radiation. Humidified air then goes to the condenser where water vapor is condensed in contact with the cooling water circulating through parallel tubes. The condensed water (fresh water) is collected at the bottom of the condenser, while brine leaves the humidifier at the bottom (Fig. 3).

2.1. Humidifier

Fig. 2(a) shows a photo of the humidifier. It is of 2 m length and 1 m width. It is composed by a 2-m^2 metal flat plate, acting as the absorber, glued on an medium density fiberboard

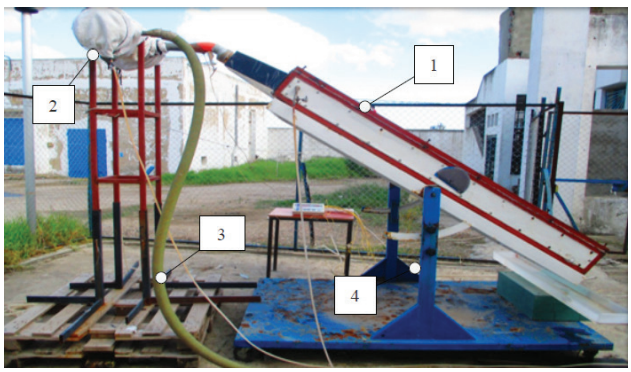

Fig. 1. Photo of the desalination unit and the experimental setup: 1 – humidifier; 2 – condenser; 3 – air suction pipe; and 4 – stand.

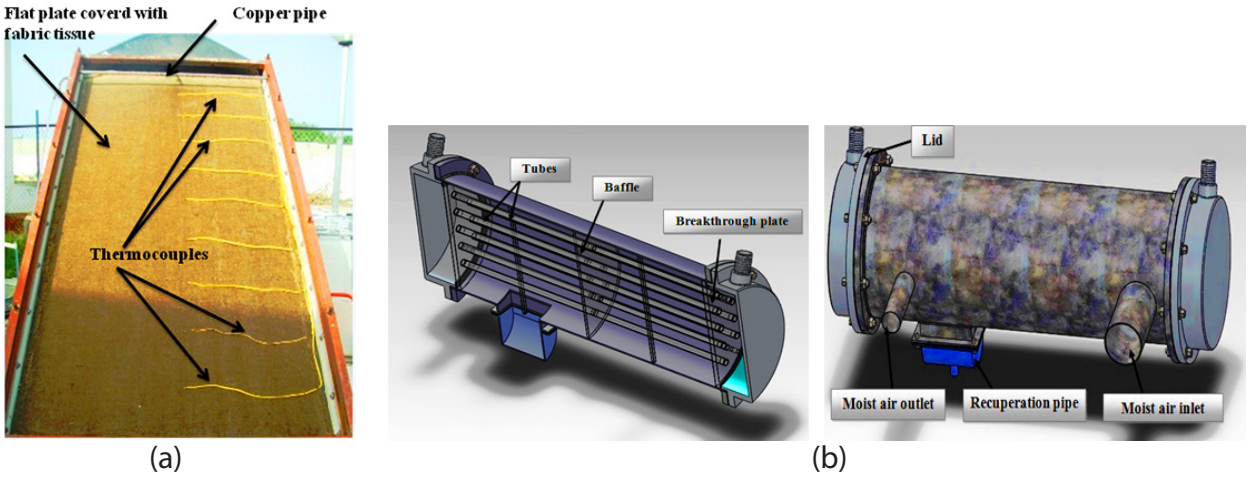

Fig. 2(a). Photo of the humidifier, and (b) Sketch of the condenser.

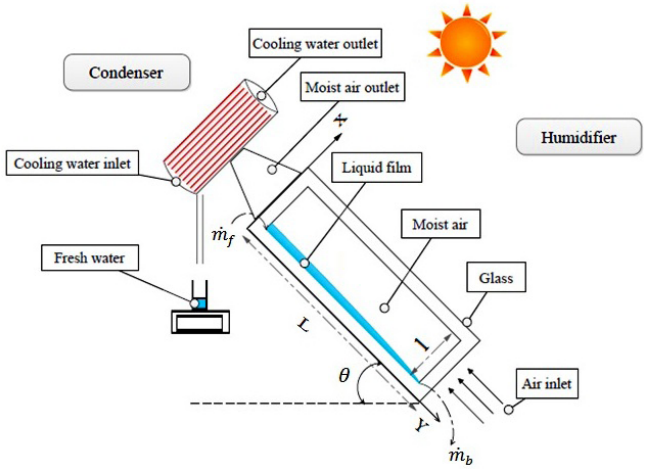

Fig. 3. Sketch of the experimental setup.

(MDF) panel. This panel is back and lateral insulated by 5 cm cork and covered by 4 cm of wooden frame. The whole is sustained by a metallic frame. A 6-mm thickness glass covers the metal plate. The distance between the plate and the glass cover was is 12 cm. Saline water is supplied to the humidifier by a constant level reservoir, which is connected to a copper pipe glued above the metal plate. This pipe is pierced with small diameter holes, which let water to fall on the plate to form a thin film. To uniformly wet the plate and avoid dry areas, a porous fabric is pasted on it, to support the liquid film. The humidifier is placed on a stand making an adjustable inclination. This inclination was set to 35°, during the experiments reported here.

2.2. Condenser

A sketch of the condenser is shown in Fig. 2(b). The condenser is a tubular heat exchanger. It is constituted by 21 copper tubes of 12 mm outside diameter, 2 mm thickness and 0.5 m length. Cooling water circulates inside these tubes. Three 4 mm thickness baffle galvanized steel plates force the passage of humid air around the copper tubes. The tubes are arranged in parallel using two breakthroughs ordinary steel plates of 4 mm thickness, which support the tubes at their ends. These plates are held securely in place using four steel rods of 0.5 m length. The outer structure of the condenser is constituted mainly of a galvanized steel shell. The shell is equipped by two pipes for the entry and exit of air stream. The shell is closed by two lids of the same material. The cooling water enters through the first cover and exits through the other. The fresh water condensate is recovered via the recuperation pipe using a recipient placed below the shell. Forced airflow in the desalination system is driven by a centrifugal fan, which is connected to the condenser outlet and operates in suction mode.

2.3. Measurement equipments

The monitoring of the solar desalination unit is achieved via a measurement system of temperature, flow rate, humidity, solar radiation and air velocity. Ten K type thermocouples are placed along the porous fabric covering the absorber plate to measure the temperature of the dripping liquid film (Fig. 2(a)). The sensors of these thermocouples are sun protected. Three other thermocouples are placed inside the condenser, to measure the inlet and the outlet cooling water temperature and humid air temperature at the inlet of the condenser. The thermocouples are connected to a data acquisition system, which store data every 5 min. Humidity and air velocity are measured using a digital multifunction device TESTO445 with capacitance and hot wire probes. An electronic balance and a stopwatch are used to measure the flow rates of feed water, brine and the condensate.

To measure the feed water flow rate $\dot{m}_f$ in the humidifier, we begin primarily by fixing the level of water in the constant level reservoir, and then we open the valve of regulation of flow placed just at the inlet of the humidifier. We wait that the surface of the fabric is wetted homogeneously. We proceed then to the feed water flow rate measurement by directing the output of the water in a beaker placed on an electronic balance. We note the mass of the beaker, which fills during the time. Thus, in absence of evaporation, the feed water flow rate merges with the brine flow rate $\dot{m}_b$. For the measurement

of the feed water flow rate, we begin the experiment early before the solar radiation reaches the humidifier.

The evaporated water flow rate is calculated by the difference between the feed water and the brine flow rates:

$$\dot{m}_{evp} = \dot{m}_f - \dot{m}_b \quad (1)$$

A weather station, installed at 3 m height near the experimental setup, records the climate parameters at every half hour: global solar radiation, ambient temperature, ambient relative humidity and wind air velocity.

Table 1 presents the technical specifications of the used sensors and probes. Air velocity is measured at the inlet of the humidifier at different positions using a hot wire anemometer. Air flow rate is then deduced from the mean velocity. Condensed fresh water and brine flow rate are indirectly measured by weighting a given mass during an interval of time. Mass is measured by an electronic balance. In order to ensure accuracy and reproducibility of the measurements, it was done at least three times during 1 h time interval. The resulting error in flow rate was found less than 0.03%.

2.4. Experimental procedure

A rigorous procedure has been followed to ensure the exactitude of the tests, especially regarding the humidifier and the measurements system. Each experiment starts early in the morning before sun radiations reach the humidifier. First, the feed water flow rate is adjusted to the desired value, which allows well wettability of the fabric that covers the humidifier absorber plate. In the case of forced air circulation, the air flow rate is adjusted to the desired value. Airflow is then measured after some minutes to ensure that steady state flow conditions are reached. Then, manual measurements are started once sun radiations reach the humidifier. These measurements concern air velocity, humidity and temperature at the humidifier entrance, as well as the liquid film temperature, brine and fresh water production. The measurements are done many times during 1 h time interval.

3. Results and discussion

3.1. Water film temperature

The temperature of the dripping liquid film in the humidifier is an important factor to understand the evaporation phenomena. Fig. 4 presents the evolution of the liquid film temperature along the absorber plate of the humidifier for different air velocities during several typical summer days at 12:00 p.m. The desalination unit runs in natural (V = 0 m/s) or forced convection (V = 1.8–5.39 m/s). We have selected several similar days in terms of meteorological conditions. y = 0 m corresponds to the liquid film entrance, while air enters the humidifier at y = 2 m. Two areas can be identified through the falling film: a first area where the liquid temperature increases. This area is a heating zone. The liquid film heats up without evaporation, which explains the increase in its temperature. This area extends over the surface from the top of the evaporator to around y = 0.4 m. This location corresponds to the maximum of the liquid film temperature. The second zone is an evaporation one, where the temperature of the liquid film decreases due to its evaporation. In this zone, the heat supplied by solar radiation is transformed into latent heat. The presence of these two zones has been reported by other authors such as Ben Jabrallah et al. [26], who studied the evaporation of a dripping water film along heated rectangular cavity walls, and Cherif et al. [27], who conducted an experimental and numerical study of water film evaporation in an open-ended vertical channel. This result was also found by Ben Radhia et al. [28] in the annular geometry.

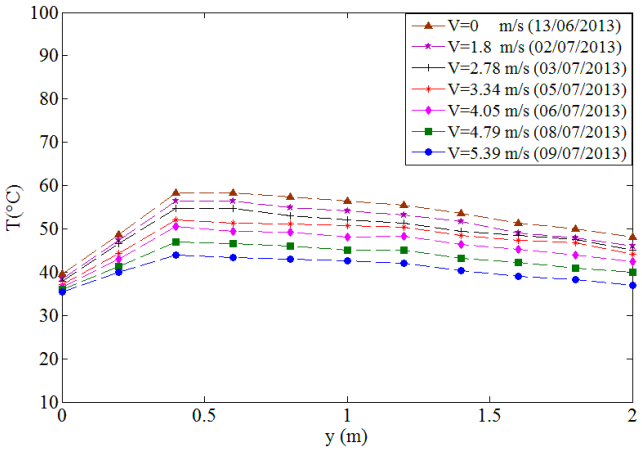

Fig. 4. Distribution of the dripping water film temperature along the humidifier for different air velocities with similar climate conditions (see Table 3 for the meteorological data).

Table 1
Technical characteristics of sensors used in the experimental setup

Sensor	Reference	Description	Uncertainty
Thermocouple	K type	Temperature	ΔT = 0.5°C
Humidity	TESTO445 capacitance probe	Relative humidity	ΔH = 2%
Velocity	TESTO445 hot wire probe	Air velocity	ΔV = 0.05 m.s^{-1}
Digital watch	–	Time	Δt = 0.2 s
Pyranometer	GL500	Global solar radiation	ΔG = 1%
Digital balance	PB1501-T2202	Mass	Δm = 0.1 g
–	–	Mass flow rate	$\frac{\Delta \dot{m}}{\dot{m}} = \left(\frac{\Delta m}{m} + \frac{\Delta t}{t}\right) = 0.03\%$

The increase of air velocity does not affect the shape of the curves but allows the cooling of liquid film. Passing from V = 0 m/s (natural convection) to higher velocities up to V = 5.39 m/s, the liquid film cools more and more. Therefore, film temperature maximum levels are lower in forced convection (V = 1.8–5.39 m/s) than in natural one (V = 0 m/s). This may be explained mainly by the increased film evaporation rate in the case of forced convection, and secondarily, the cooling effect of the liquid film induced by the forced airflow.

Fig. 5 shows time evolution of the liquid film temperature during the day for different air velocities at y = 0.4 m. The profiles of liquid film temperatures during the day exhibit the same shape in forced convection (V = 1.8–5.39 m/s) than in natural one (V = 0 m/s). In the beginning of the day, the film temperature increases as a result of the increasing of solar irradiation. For the remaining of the day, the liquid film temperature decreases following the decrease in solar irradiation in the afternoon. Fig. 6 confirms the result found in Fig. 4. The liquid film temperatures during the day decreases increasingly passing from natural (V = 0 m/s) to forced convection (V = 1.8–5.39 m/s).

3.2. Evaporated and condensed flow rate

Figs. 6 and 7 show the evolution of the water evaporated/condensed flow rate and the global solar irradiation during two similar summer days in natural and forced convection. Time evolution of the evaporated/condensed water flow rate has the same behavior than that of the solar irradiation with 1 h shift, due to the system thermal inertia. Indeed, its maximum occurs at 2:00 p.m. while that of the global solar irradiation occurs at 1:00 p.m. Comparison of evaporated water flow rate profiles for natural and forced convection (Fig. 6) and those corresponding to condensed flow rate (Fig. 7) shows that forced convection increases film evaporation by about 30% and condensation of water vapor inside the condenser by nearly 35%. Although, forced convection lowers water film temperature, and then its evaporation rate, in comparison with the buoyancy-driven airflow, as stated in the previous subsection (Figs. 4 and 5). Such results were also reported by Wang et al. [17].

In order to point out the effect of ambient air humidity on the HDH desalination unit production, many experiments were conducted during several days of June 2013 with different ambient air humidity. Table 2 presents some meteorological data of these days. Fig. 8 shows the cumulative fresh water production during these days, in the case of natural convection operation mode. The overall fresh water production of the desalination unit is 4.5 kg/d for 13th June with ambient air humidity in the range of 43%–57%. Fresh water production decreases to 3.8 kg in 12th June with ambient air humidity ranging from 60% to 72%. This decreasing is around 18%.

To study the influence of air velocity on the production of the desalination system, experiments were conducted during several days of June and July 2013 that are characterized by similar climate conditions (Table 3). Fig. 9 shows the fresh water production during the day for different air velocity.

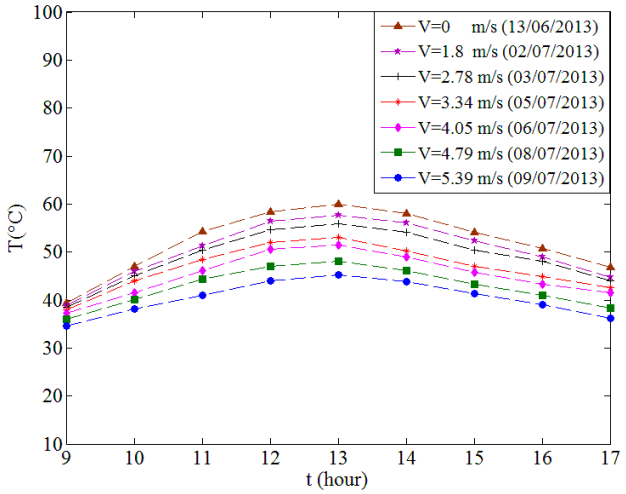

Fig. 5. Evolution of the liquid film temperature in the humidifier during the day for different air velocities with similar climate conditions (see Table 3 for the meteorological data).

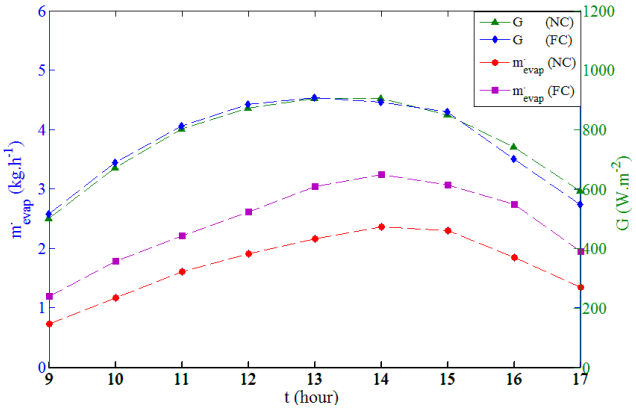

Fig. 6. Evolution of the evaporated flow rate and the global solar irradiation in: (i) natural convection (NC: 13th June 2013, G_{av} = 760.6 W.m^{-2}, T_{amb} = 26°C–36°C, H_{amb} = 43%–57%, $\dot{m}_f$ = 4.1 kg.h^{-1}) and (ii) forced convection (FC: 5th July 2013, G_{av} = 758.4 W.m^{-2}, T_{amb} = 24°C–35°C, H_{amb} = 45%–61%, $\dot{m}_f$ = 4.1 kg.h^{-1}, V = 3.34 m.s^{-1}).

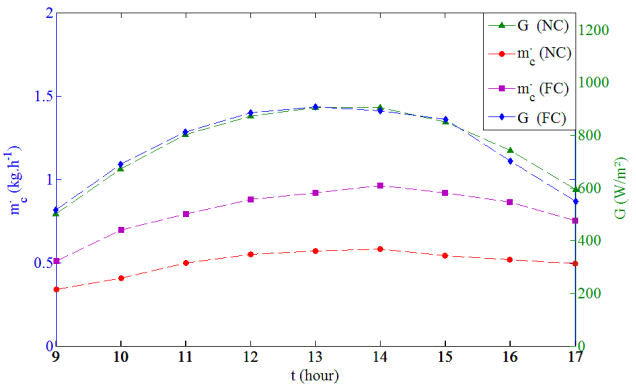

Fig. 7. Evolution of the condensed water flow rate and the global solar irradiation in: (i) natural convection (NC: 13th June 2013, G_{av} = 760.6 W.m^{-2}, T_{amb} = 26°C–36°C, H_{amb} = 43%–57%, $\dot{m}_f$ = 4.1 kg.h^{-1}) and (ii) forced convection (FC: 5th July 2013, G_{av} = 758.4 W.m^{-2}, T_{amb} = 24°C–35°C, H_{amb} = 45%–61%, $\dot{m}_f$ = 4.1 kg.h^{-1}, V = 3.34 m. s^{-1}).

Table 2
Weather conditions for different days of measurements

Day	H (%)	T_{amb} (°C)	G_{av} (W.m^{-2})
12/06/2013	58–70	19–28	705.4
13/06/2013	43–57	26–36	760.6
15/06/2013	47–59	23–33	731.9
16/06/2013	49–60	21–31	728.1
17/06/2013	52–68	20–30	715.9

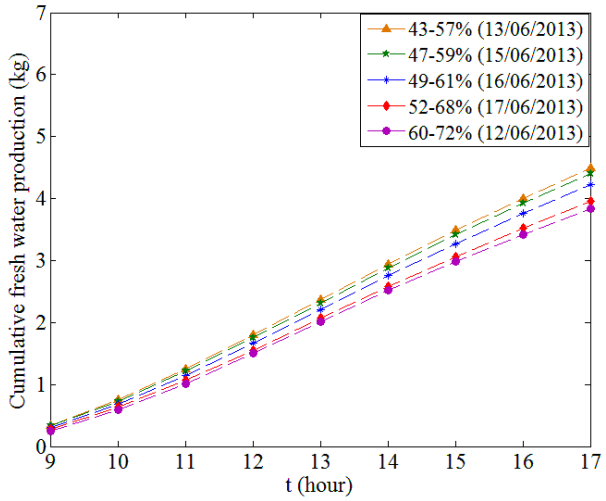

Fig. 8. Time evolution of the cumulative fresh water production in natural convection during several days with different ambient humidity (see Table 2 for the meteorological data).

Table 3
Weather data for different days of measurements with similar climate conditions

Day	H (%)	T_{amb} (°C)	G_{av} (W.m^{-2})
13/06/2013	43–58	26–36	760.6
02/07/2013	43–59	25–36	759.1
03/07/2013	44–63	26–34	755.7
05/07/2013	45–61	24–35	758.4
06/07/2013	40–55	28–37	771.5
08/07/2013	48–63	26–34	754.6
09/07/2013	44–62	25–34	756.8

The case of natural convection is also reported (V = 0). Fresh water production increases up to V = 3.34 m/s. This increase is due to the improved evaporation by the forced convection. Beyond this value, daily cumulated fresh water production decreases abruptly. In fact, as air velocity exceeds 3.34 m/s, residence time of humid air inside the condenser drops and water vapor has not enough time to exchange heat with the cooling water even if they are abundant because they are sucked. It is interesting to mention that daily fresh water production at V = 4.79 m.s^{-1} is essentially similar to that of free convection case, while for V = 5.79 m.s^{-1}, fresh water production falls below that of the buoyancy-driven airflow. The

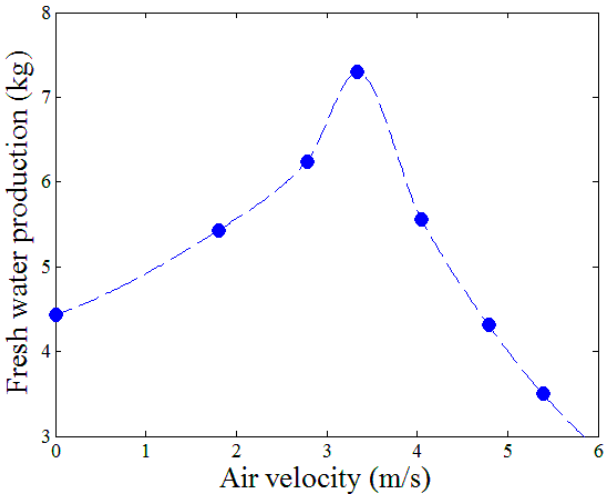

Fig. 9. Effect of air velocity on the daily fresh water production of the desalination system for similar climate conditions (see Table 3 for the meteorological data).

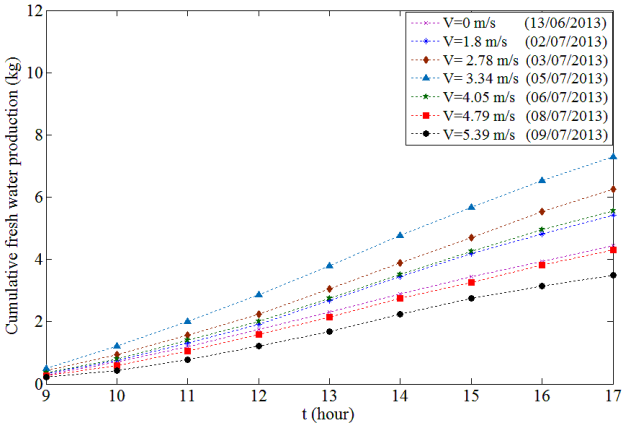

Fig. 10. Time evolution of the cumulative fresh water production for different air velocities with similar climate conditions (see Table 3 for the meteorological data).

previous results are confirmed by Fig. 10, where the cumulative fresh water production along the day is presented for different air velocities. The maximum production of the desalination unit was reached on 5th July 2013, and it was 7.29 kg of fresh water for air velocity 3.34 m/s. The production of this unit is acceptable compared with desalination units by HDH with small scale. For example, the maximum production of Nafey et al. [13] in comparable climatic conditions is almost 8 kg/d and Nawayseh et al. [29] is of 7.5 kg/d.

3.3. Gained output ratio

One of the most important parameters for the evaluation of the energy performance of the desalination units is the GOR. It is defined as the ratio of the latent heat of condensation of the distillate water produced to the total heat input absorbed by the humidifier [7,8,23,30]. This parameter is an index of the amount of heat recovery in the desalination unit. GOR is given by the following expression [30]:

$$\mathrm{GOR} = \frac{\dot{m}_c \cdot h_{fg}}{\dot{Q}_{in}} \quad (2)$$

where latent heat of condensation h_{fg} is evaluated at the mean temperature of the condensate as follows [31]:

$$h_{fg} = 2501.897149 - 2.407064037T + 1.192217 \times 10^{-3}T^2 - 1.5863 \times 10^{-5}T^3 \quad (3)$$

where T is in k and h_{fg} in kJ/kg.

Q_{in} is the part of the global solar irradiation absorbed by the water film (i.e., total solar irradiation received by the humidifier glass minus thermal losses). It is given by the following equation:

$$\dot{Q}_{in} = \alpha_t \mathrm{GS} \quad (4)$$

where α_t is the apparent absorptivity of the water film [32]:

$$\alpha_t = \tau_g \alpha_b + \tau_g \tau_b \alpha_p \quad (5)$$

where τ_g and τ_b are, respectively, the transmissivity of the glazing and brine. α_p and α_b are the absorptivity of the absorber plate and brine, respectively. With $\tau_g = 0.9$, $\tau_b = 0.68$, $\alpha_p = 0.95$ and $\alpha_b = 0.3$ [33].

Fig. 11 presents time evolution of the GOR during the two similar summer days as in Fig. 9, in natural and forced convection. The global solar irradiation is also reported. Comparison of GOR for natural and forced convection shows that forced convection increases GOR by almost 39%. This is, essentially, due the condensation increase mentioned above. In the case of natural convection, the GOR changes between 0.3 at 9:00 a.m. and 0.39 at 2:00 p.m.; while for forced convection, it evolves between 0.55 and 0.65.

The GOR maxima achieved for different air velocities are shown in Fig. 12. These values correspond to similar meteorological conditions for selected days of June and July 2013. Obviously, the best thermal performances are reached for the optimal air velocity $V = 3.34$ m/s. The values of GOR seems weak indicating that energy performances of the desalination unit are somewhat poor, even if air is circulated in a forced way with the optimal velocity. Indeed, the maximum of GOR is 0.65, while the reported values of GOR in the literature are 3 in [22] and 4 or 2.6, respectively, with or without mass extraction in [8]. Narayan et al. [7] discussed this point in their well-documented review paper. It is of importance to mention that the studied desalination unit is an open-air and open-water one without water heating, while the desalination units studied by Nayaran et al. [8] and by Zhani and Ben Bacha [22] have closed-air and open-water loops. In addition, in both these units, salt water is preheated in the condenser (heat recovery) and then heated in a solar water collector [22] or an electric heater [8]. On the other hand, as the humidifier works well (see next section), it is believed that the main reason of the GOR weak values is due to low performances of the condenser. Despite the fact that heat recovery is not used here (latent heat of condensation is lost in the open cooling water circuit), it was observed during the experimental tests that some of the desalination unit parameters are not at their optimal values. The most important parameter is the feeding saline water flow rate. Indeed, Zhani [23] reported that, in the cooling tower type humidifier, there is an optimal value of this flow rate. The author results display GOR = 0.5 for low feeding water flow rates and GOR = 2 for high feeding water flow rates, while the optimal value of GOR is 3. These points are under consideration for future improvements of the desalination unit.

3.4. Thermal efficiency of the humidifier

The thermal efficiency of the humidifier was evaluated by comparing the overall energy gained by the humidified air and the falling water film with the total solar flux:

$$\eta = \frac{(\dot{m}_{air} c_{pair} + \dot{m}_{air}(\omega_{out} - \omega_{in}) c_{pv}).(T_{air,out} - T_{air,in}) + \dot{m}_f c_{pf}(T_{f,out} - T_{f,in})}{G.S} \quad (6)$$

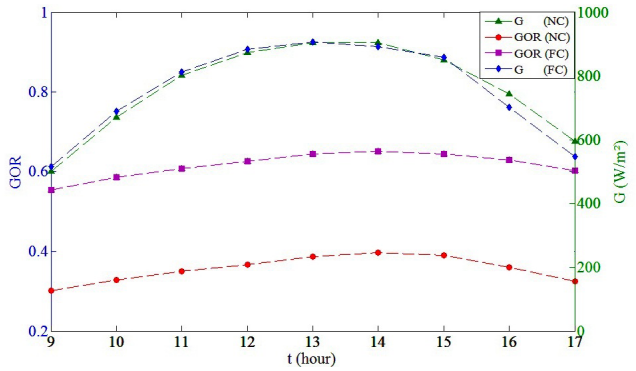

Fig. 11. Evolution of the gained output ratio (GOR) and the global solar irradiation around a day in: (i) natural convection (NC: 13th June 2013, G_{av} = 760.6 W.m^{-2}, T_{amb} = 26°C–36°C, H_{amb} = 43%–57 %, $\dot{m}_f$ = 4.1 kg.h^{-1}) and (ii) forced convection (FC: 5th July 2013, G_{av} = 758.4 W.m^{-2}, T_{amb} = 24°C–35°C, H_{amb} = 45%–61%, $\dot{m}_f$ = 4.1 kg.h^{-1}, V = 3.34 m.s^{-1}).

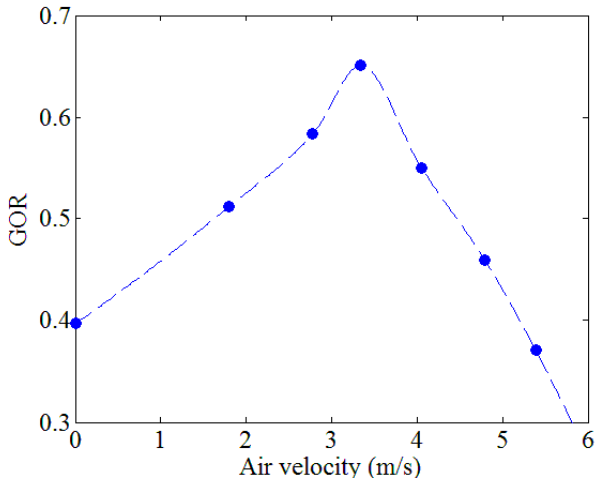

Fig. 12. Variation of the GOR of the desalination system with air velocities.

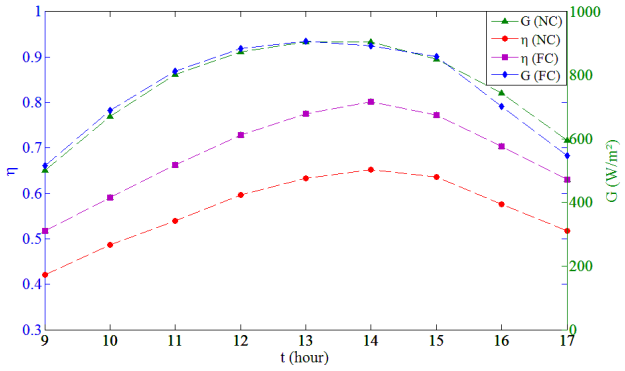

Fig. 13. Time evolution of the thermal efficiency of the humidifier during 2 d with similar climate conditions, in: (i) natural (NC: 13th June 2013, G_{av} = 760.6 W.m^{-2}, T_{amb} = 26°C–36°C, H_{amb} = 43%–57%, $\dot{m}_f$ = 4.1 kg.h^{-1}) and (ii) forced convection (FC: 5th July 2013, G_{av} = 758.4 W.m^{-2}, T_{amb} = 24°C–35°C, H_{amb} = 45%–61%, $\dot{m}_f$ = 4.1 kg.h^{-1}, V = 3.34 m.s^{-1}).

Specific humidity of humid air is evaluated by using the perfect gas assumption [23]:

$$\omega = \frac{0.622.P_{v\_sat}(T)}{P_{atm} - P_{v\_sat}(T)} \quad (7)$$

where P_{atm} is the atmospheric pressure, and P_{v_sat} is the saturation pressure of water.

P_{v_sat} is computed from the following equation [28]:

$$\log(P_{v\_sat}) = 28.590521 - 8.2 \times \log(T) + 2.4804.10^{-3} \times T - \frac{3142.32}{T} \quad (8)$$

where T is in K and P_{v_sat} in atm.

Time variation of the humidifier thermal efficiency is depicted in Fig. 13 for both free and forced convection during two similar meteorological conditions days. It can be seen that high efficiency is achieved mainly for forced convection. Indeed, thermal efficiency changes during the day between 52% and 80% in the case of forced convection, while it evolves between 40% and 63% in the case of free convection. It can be concluded that the humidifier works well. Furthermore, forced airflow improves thermal efficiency of the humidifier by at least 25%. This improvement is due to the high water film evaporation flow rate induced by forced convection as mentioned in the previous sections (Fig. 6). As the considered humidifier configuration is rare in the literature, it is difficult to compare the present work with previous ones. However, it is interesting to mention that Narayan et al. [7] performed thermal performance comparison of solar air heaters used in desalination systems through analysis of 13 papers.

4. Conclusion

An experimental study of a solar desalination bench-scale unit that operates with the HDH process is performed. The unit has been tested on real site of Bizerte (Tunisia), and it was monitored during several days of summer 2013. The existence of the heating and the evaporation zones along the humidifier plate, which supports the salted water film, has been pointed out either in natural and forced convection. These results show improvements of the evaporated and condensed water flow rates by forced convection compared with natural convection. The optimal value of air velocity for which the unit produces the maximum of fresh water has been determined. It was stated as 3.34 m/s, which leads to 7.29 kg/d of fresh water for the climate conditions of the 5th July 2013. Thermal performances of the desalination unit are studied in terms of the GOR, which is an index of the amount of the heat recovery in the desalination unit, and the humidifier thermal efficiency. The air–water humidifier performs well with 80% thermal efficiency in the case of forced convection, while the GOR of the studied unit exhibits low values due to low energy performances of the condenser. This point is under consideration for improvements.

Acknowledgment

Financial support of the Morocco-Tunisia Cooperation Program, Action Intégrée ref. 12-MT-05, is acknowledged.

Symbols

c_{pair}	—	Specific heat of dry air, J.kg^{-1}.K^{-1}
c_{pf}	—	Specific heat of feeding water, J.kg^{-1}.K^{-1}
c_{pv}	—	Specific heat of water vapor, J.kg^{-1}.K^{-1}
G	—	Global solar irradiation, W.m^{-2}
H	—	Relative humidity, %
h_{fg}	—	Latent heat of vaporization, J.kg^{-1}
l	—	Width of the humidifier, m
L	—	Length of the humidifier, m
$\dot{m}$	—	Mass flow rate, kg.s^{-1}
P_v	—	Vapor pressure, Pa
Q_{in}	—	Solar power absorbed by water film, W
S	—	Glass surface of the humidifier, m^2
t	—	Time, s
T	—	Temperature, °C
V	—	Air velocity, m.s^{-1}
y	—	Coordinate in the flow direction, m

Greek

α	—	Absorptivity
θ	—	Inclination angle of the humidifier
ω	—	Specific humidity, $kg_{water}/kg_{dry\ air}$
τ	—	Transmissivity

Subscripts

air	—	Dry air
amb	—	Ambient
atm	—	Atmospheric
av	—	Average
b	—	Brine
c	—	Condensate
evap	—	Evaporated
f	—	Feed water
g	—	Glass
in	—	Inlet
out	—	Outlet
p	—	Absorber plate of humidifier.
sat	—	Saturation

Acronyms

FC	—	Forced convection
GOR	—	Gained output ratio (ratio of the total latent heat of condensation of the produced freshwater to the input thermal energy)
HDH	—	Humidification-dehumidification
NC	—	Natural convection

References

[1] L. Garcia-Rodriguez, Seawater desalination driven by renewable energies: a review, Desalination, 143 (2002) 103–l13.

[2] A.A. Abufayed, M.K.A. Elghuel, M. Rashed, Desalination: a viable supplemental source of water for the arid states of North Africa, Desalination, 152 (2003) 75–81.

[3] F. BenJemaa, I. Houcine, M.H. Chahbani, Potential of renewable energy development for water desalination in Tunisia, Renew. Energy, 18 (1999) 331–347.

[4] D. Zejli, A. El-Midaoui, Moroccan Potentialities of Renewable Energy Sources for Water Desalination, L. Rizzuti, H.M. Ettouney, A. Cipollina, Eds., Solar Desalination for the 21st Century, Part of the NATO Security through Science Series, Springer, 2007, pp. 127–138.

[5] N. Ghaffour, V.K. Reddy, M. Abu-Arabi, Technology development and application of solar energy in desalination: MEDRC contribution, Renew. Sustain. Energy Rev., 15 (2011) 4410–4415.

[6] N. Ghaffour, S. Lattemann, T. Missimer, K.C. Ng, S. Sinha, G. Amy, Renewable energy-driven innovative energy-efficient desalination technologies, Appl. Energy, 136 (2014) 1155–1165.

[7] G.P. Narayan, M.H. Sharqawy, E.K. Summers, J.H. Lienhard, S.M. Zubair, M.A. Antar, The potential of solar-driven humidification–dehumidification desalination for small-scale decentralized water production, Renew. Sustain. Energy Rev., 14 (2010) 1187–1201.

[8] G.P. Narayan, M.G.S. John, S.M. Zubair, J.H. Lienhard, Thermal design of the humidification dehumidification desalination system: an experimental investigation, Int. J. Heat Mass Transfer, 58 (2013) 740–748.

[9] N.K. Nawayseh, M.M. Farid, S. Al-Hallaj, A.R. Al-Timimi, Solar desalination based on humidification process—I. Evaluating the heat and mass transfer coefficients, Energy Convers. Manage., 40 (1999) 1423–1439.

[10] N.K. Nawayseh, M.M. Farid, A.A. Omar, A. Sabirin, Solar desalination based on humidification process—II. Computer simulation, Energy Convers. Manage., 40 (1999) 1441–1461.

[11] Y.J. Dai, H.F. Zhang, Experimental investigation of a solar desalination unit with humidification and dehumidification, Desalination, 130 (2000) 169–175.

[12] A.S. Nafey, H.E.S. Fath, S.O. El-Helaby, A.M. Soliman, Solar desalination using humidification dehumidification processes. Part I: A numerical investigation, Energy Convers. Manage., 45 (2004) 1243–1261.

[13] A.S. Nafey, H.E.S. Fath, S.O. El-Helaby, A.M. Soliman, Solar desalination using humidification–dehumidification processes. Part II. An experimental investigation, Energy Convers. Manage., 45 (2004) 1263–1277.

[14] J. Orfi, M. Laplante, H. Marmouch, N. Galanis, B. Benhamou, S. Ben Nasrallah, C.T. Nguyen, Experimental and theoretical study of a humidification dehumidification water desalination system using solar energy, Desalination, 168 (2004) 151–159.

[15] C. Yamale, I. Solmus, A solar desalination system using humidification–dehumidification process: experimental study and comparison with the theoretical results, Desalination, 220 (2008) 538–551.

[16] H. Marmouch, J. Orfi, S. Ben Nasrallah, Effect of a cooling tower on a solar desalination system, Desalination, 238 (2009) 281–289.

[17] J.H. Wang, N.Y. Gao, Y. Deng, Y.L. Li, Solar power-driven humidification–dehumidification (HDH) process for desalination of brackish water, Desalination, 305 (2012) 17–23.

[18] A.E. Kabeel, M.H. Hamed, Z.M. Omara, S.W. Sharshir, Experimental study of a humidification-dehumidification solar technique by natural and forced air circulation, Energy, 68 (2014) 218–228.

[19] C. Yildirim, S.K. Soylu, I. Atmaca, I. Solmus, Experimental investigation of a portable desalination unit configured by a thermoelectric cooler, Energy Convers. Manage., 85 (2014) 140–145.

[20] T. Tahri, M. Douani, M. Amoura, A. Bettahar, Study of influence of operational parameters on the mass condensate flux in the condenser of seawater greenhouse at Muscat, Oman, Desal. Wat. Treat., 57 (2016) 13930–13937.

[21] N. Niroomand, M. Zamen, M. Amidpour, Theoretical investigation of using a direct contact dehumidifier in humidification–dehumidification desalination unit based on an open air cycle, Desal. Wat. Treat., 54 (2015) 305–315.

[22] K. Zhani, H. Ben Bacha, Experimental investigation of a new solar desalination prototype using the humidification dehumidification principle, Renew. Energy, 35 (2010) 2610–2617.

[23] K. Zhani, Solar desalination based on multiple effect humidification process: thermal performance and experimental validation, Renew. Sustain. Energy Rev., 24 (2013) 406–417.

[24] K. Zhani, H. Ben Bacha, T. Damak, Modeling and experimental validation of a humidification-dehumidification desalination unit solar part, Energy, 36 (2011) 3159–3169.

[25] S. Saidi, R. Ben Radhia, B. Dhifaoui, S. Ben Jabrallah, Experimental study of the inclined solar film evaporator, Desal. Wat. Treat., 56 (2015) 2576–2583.

[26] S. Ben Jabrallah, A.S. Cherif, B. Dhifaoui, A. Belghith, J.P. Corriou, Experimental study of the evaporation of a falling film in a closed cavity, Desalination, 180 (2005) 197–206.

[27] A.S. Cherif, M.A. Kassim, B. Benhamou, S. Harmand, J.P. Corriou, S. Ben Jabrallah, Experimental and numerical study of mixed convection heat and mass transfer in a vertical channel with film evaporation, Int. J. Therm. Sci., 50 (2011) 942–953.

[28] R. Ben Radhia, J.P. Corriou, S. Harmand, S. Ben Jabrallah, Numerical study of evaporation in a vertical annulus heated at the inner wall, Int. J. Therm. Sci., 50 (2011) 1996–2005.

[29] N.K. Nawayseh, M.M. Farld, A.A. Omar, S.M. Al-Hallaj, A.R. Tamimi, A simulation study to improve the performance of a solar humidification-dehumidification desalination unit constructed in Jordan, Desalination, 109 (1997) 277–284.

[30] J. Koschikowski, M. Wieghaus, M. Rommel, Solar thermal-driven desalination plants based on membrane distillation, Desalination, 156 (2003) 295–304.

[31] G. Al-Enezi, H. Ettouney, N. Fawzy, Low temperature humidification dehumidification desalination process, Energy Convers. Manage., 47 (2006) 470–484.

[32] C. Khelif, B. Touati, Characterization of a greenhouse distiller, Review of Renewable Energies, 1 (1998) 99–108.

[33] M. Zerrouki, N. Settou, Y. Marif, M.M. Belhadj, Simulation study of a capillary film solar still coupled with a conventional solar still in south Algeria, Energy Convers. Manage., 85 (2014) 112–119.